## Title
THE REACTION n+p _> <*>6A ++ AT 2.3 AND 2.67 GeV/c



Authors
Kb, W.
Gidal, G.
Grether, D.F.

Publication Date
1970-08-01

Submitted to the XVth International Conference on High Energy Physics Kiev, USSR. Aug. 26-Sept. 4, 1970.

UCRL-19779
Preprint c. 2



# THE REACTION $\pi^+ p \rightarrow \omega^0 \Delta^{++}$ AT 2.3 AND 2.67 GeV/c

W. Ko, G. Gidal, and D. F. Grether

August 1970

AEC Contract No. W-7405-eng-48



LAWRENCE RADIATION LABORATORY
UNIVERSITY of CALIFORNIA BERKELEY

UCRL-19779

UCRL-19779

Submitted to the XVth International
Conference on High Energy Physics
Kiev, 1970

# THE REACTION $\pi^+ p \to \omega^0 \Delta^{++}$ AT 2.3 AND 2.67 GeV/c

W. Ko, G. Gidal, and D. F. Grether

Lawrence Radiation Laboratory
University of California
Berkeley, California

August 1970

We present preliminary results on the reaction

$$\pi^+ p \rightarrow \omega^o \Delta^{++}(1238) \qquad (1)$$

at 2.3 and 2.67 GeV/c. The data is from some 450 000 exposures of the Lawrence Radiation Laboratory 25-inch hydrogen bubble chamber which yielded about 16 000 four-prong events at 2.3 GeV/c and about 37 000 at 2.67 GeV/c. The events were measured on the Flying Spot Digitizer (FSD) and processed through the FOG-CLOUDY-FAIR system. Kinematic ambiguities were resolved on the basis of the automatic ionization measurements available from the FSD.[1] Events satisfying the 1-c hypothesis

$$\pi^+ p \rightarrow \pi^+ p \, \pi^+ \pi^- \pi^o \qquad (2)$$

were additionally constrained to the 2-c hypothesis

$$\pi^+ p \rightarrow \pi^+ p \, \omega^o, \quad \omega^o \rightarrow \pi^+ \pi^- \pi^o$$

$\omega^o$ events were chosen by the criterion

$$\chi^2(2c) - \chi^2(1c) \leq 10$$

For "double" $\omega^o$ events, the combination with the smallest $\chi^2(2c)$ was selected.

Figure 1 shows the $\pi^+\pi^-\pi^0$ invariant mass distributions. The unshaded part of the histogram represents the number of $\omega^0$ events selected in each mass region. Fig. 1 also shows the mass distributions of the $\pi^+p$ combinations recoiling off the $\omega^0$. The dotted curve represents our estimate of the background under the $\Delta^{++}$ peak and was used in the determination of the $\omega^0\ \Delta^{++}$ cross section. The $\Delta^{++}$ mass band is defined as $1.16\ \text{GeV} \leq M(p\pi^+) \leq 1.28\ \text{GeV}$. The above criteria for $\omega^0$ and $\Delta^{++}$ yield 1692 events at 2.3 and 3497 at 2.67 GeV/c.

We determine the total cross section for reaction (1) to be $.72 \pm .10$ mb at 2.3 GeV/c and $.81 \pm .08$ mb at 2.67 GeV/c. The differential cross sections are shown in Fig. 2. While the Regge Pole model is most easily tested in reactions where only a single trajectory is exchanged in the t-channel, the absence[2] of a dip near $t = -.5$ in the differential cross section for reaction (2) indicates that both natural ($\rho$) and unnatural (B) parity trajectories are exchanged.

Several attempts have been made[3,4,5] to extract these exchange contributions for reaction (2). For example, the assymptotic relation $\rho_{1-1} = -\rho_{11}$ should be satisfied at the value of t where the $\rho$ exchange contribution vanishes or, more practically, the combination $\sigma_1^+ \equiv \rho_{11} + \rho_{1-1}$ should exhibit a minimum. In a like manner $\sigma_1^- \equiv \rho_{11} - \rho_{1-1}$ and $\rho_{00}$ measure the B exchange contribution. These combinations of spin density matrix elements together with $\sigma_1^+ \frac{d\sigma}{dt}$ and $\rho_{00} \frac{d\sigma}{dt}$ are shown in Figs. 1-3. Several indications of dips in these combinations have been given in Refs. 3-5. Some structure is also seen in this experiment, although this is always more pronounced at 2.67 GeV/c than at 2.3 GeV/c. In particular, at 2.67 GeV/c we see evidence for a dip in $\rho_{00}$, $\rho_{00}\frac{d\sigma}{dt}$ and $\sigma_1^-$ near t = -0.8 as reported in Ref. 4. The natural parity combinations $\sigma_1^+$ and $\sigma_1^+\frac{d\sigma}{dt}$ show evidence for a dip near t = -0.6 though this evidence is rather weak. Such evidence was also reported in Ref. 5 at a somewhat larger t value. The interpretation of the combinations $\rho_{11} \pm \rho_{1-1}$ is complicated by the fact that $\rho_{1-1}$ fluctuates about zero, possibly causing the fluctuations observed in $\sigma_1^{\pm}$ between t = -0.8 and t = -1.0. A dip in $\rho_{00}$ is observed near t = -0.3 as was reported in Ref. 5.

Thews[6] has proposed a test for the exchange of a single trajectory. For reaction (2) the inequality

$$\frac{x^2-1}{x^2+1} \leq \frac{|\rho_{1\,-1}|}{\rho_{11}} \leq 1 \quad ; \quad x = \cos\theta_t$$

must be satisfied. We show the results of this test in Fig. 4 and note that for most values of t the points lie outside the limits indicating the presence of both natural and unnatural parity exchanges.

In the Quark model of Bialas and Zalewski,[7] the additivity of quark-quark amplitudes, with no other assumption, gives the following relation between the decay density matrix elements of $\omega$ and $\Delta$:

$$\rho_{11} + \rho_{1\,-1} = \frac{4}{3}\,\rho_{\frac{3}{2}\frac{3}{2}} + \frac{4}{\sqrt{3}}\,\mathrm{Re}\,(\rho_{\frac{3}{2}\,-\frac{1}{2}})$$

The good agreement of this relation is shown in Fig. 5.

With additional assumptions of the quark-quark amplitude that $\langle +-|-+\rangle = \langle -+|+-\rangle$ we have the following relation

$$\rho_{11} = \frac{4}{3}\ \rho_{\frac{3}{2}\frac{3}{2}} \quad ; \quad \rho_{1\,-1} = \frac{4}{\sqrt{3}}\ \mathrm{Re}\left(\rho_{\frac{3}{2}\,-\frac{1}{2}}\right) \quad \mathrm{Re}\left(\rho_{10}\right) = \frac{4}{\sqrt{6}}\ \mathrm{Re}\left(\rho_{\frac{3}{2}\frac{1}{2}}\right)$$

These relations are frame dependent. Figs. 6 and 7 show these relations in the s and t channel helicity frames (i.e. helicity and Jackson frames, respectively). Excellent agreement is again demonstrated.

The further assumption that $\langle ++|--\rangle = \langle --|++\rangle$ implies that $\mathrm{Re}(\rho_{10}) = 0$ and $\mathrm{Re}\ (\rho_{\frac{3}{2}\frac{1}{2}}) = 0$. Fig. 8 demonstrates that these relations do not agree with the experiment.

We have shown here the excellent agreement of the first two classes of relations at this low energy experiment. It was, however, pointed out by Maor[8] that the same relations can be obtained at the small t region by Regge theory if one assumes (1) the factorization of the Regge residue; (2) the dipole coupling of the natural parity exchange at the $\Delta$ vertex; and (3) the non-spin flip of the unnatural parity exchange.

## REFERENCES

1. G. Borreani, D. Hall, L. Shalz, and P. Hanson, in Proceedings of the International Conference on Advanced Data Processing for Bubble and Spark Chambers, Argonne, 1968; and University of California Lawrence Radiation Laboratory Report UCRL-18545 (1968), unpublished.

2. See, e.g., D. Brown, et al., Phys. Rev. Letters 19, 664 (1967).

3. H. Hogaasen and H. J. Lubatti, Phys. Rev. Letters 26B, 166 (1968); J. P. Ader, M. Capdeville, G. Cohen-Tannoudji, Ph. Salin, Nuovo Cimento 56A, 952 (1968).

4. D. Brown et al., UCRL-18351 (1968), and Phys. Rev. D1, 3053 (1970).

5. G. S. Abrams et al., UCRL-19743 (1970).

6. R. L. Thews, Phys. Rev. 188, 2264 (1969).

7. A. Bialas and K. Zalewski, Nuclear Physics B6, 465 (1968).

8. U. Maor, Nuclear Physics B19, 20 (1970).

# FIGURE CAPTIONS

Fig. 1. $\pi^+\pi^-\pi^o$ mass distributions and mass distribution of $\pi^+p$ combinations at 2.3 and 2.67 GeV/c. The unshaded portion of the $M(\pi^+\pi^-\pi^o)$ histogram represents the number of events selected as $\omega^o$'s. The dotted curves on the $M(\pi^+p)$ distributions are three-body phase space normalized to the number of events above 1.35 GeV.

Fig. 2. $d\sigma/dt$ and $\rho_{oo}$ $d\sigma/dt$ for $\pi^+p \to \omega^o \Delta^{++}$ at 2.3 and 2.67 GeV/c.

Fig. 3. Spin density matrix elements in the Jackson frame for $\pi^+p \to \omega^o \Delta^{++}$ at 2.3 and 2.67 GeV/c.

Fig. 4. Combinations $\rho_{11} \pm \rho_{1\,-1}$ and $\rho_{11} + \rho_{1\,-1}$ $d\sigma/dt$ for $\pi^+p \to \omega^o \Delta^{++}$ at 2.3 and 2.67 GeV/c.

Fig. 5. Ratio $|\rho_{1\,-1}| / \rho_{11}$ together with upper and lower bounds discussed in text.

Fig. 6. Comparison of $\rho_{11} + \rho_{1\,-1}$ of the $\omega$ decay with $\frac{4}{3}\rho_{\frac{3}{2}\frac{3}{2}} + \frac{4}{\sqrt{3}}\,\mathrm{Re}\left(\rho_{\frac{3}{2},\,-\frac{1}{2}}\right)$ of the $\Delta$ decay for 2.30 and 2.67 BeV/c.

Fig. 7. Helicity frame comparison of $\rho_{11}$ with $\frac{4}{3}\rho_{\frac{3}{2}\frac{3}{2}}$, $\rho_{1,\,-1}$ with $\frac{4}{\sqrt{3}}\,\mathrm{Re}\left(\rho_{\frac{3}{2},\,-\frac{1}{2}}\right)$ and $\mathrm{Re}\,(\rho_{10})$ with $\frac{4}{\sqrt{6}}\,\mathrm{Re}\left(\rho_{\frac{3}{2}\,\frac{1}{2}}\right)$.

Fig. 8. Jackson frame comparison of $\rho_{11}$ with $\frac{4}{3}\rho_{\frac{3}{2}\frac{3}{2}}$, $\rho_{1\,-1}$ with $\frac{4}{3}\,\mathrm{Re}\left(\rho_{\frac{3}{2},\,-\frac{1}{2}}\right)$ and $\mathrm{Re}\,(\rho_{10})$ with $\frac{4}{\sqrt{6}}\,\mathrm{Re}\left(\rho_{\frac{3}{2}\,\frac{1}{2}}\right)$.

Fig. 9. Comparison of quantities Re $(\rho_{10})$ and Re $\left(\rho_{\frac{3}{2}\frac{1}{2}}\right)$ with 0 in both Jackson and helicity frames.

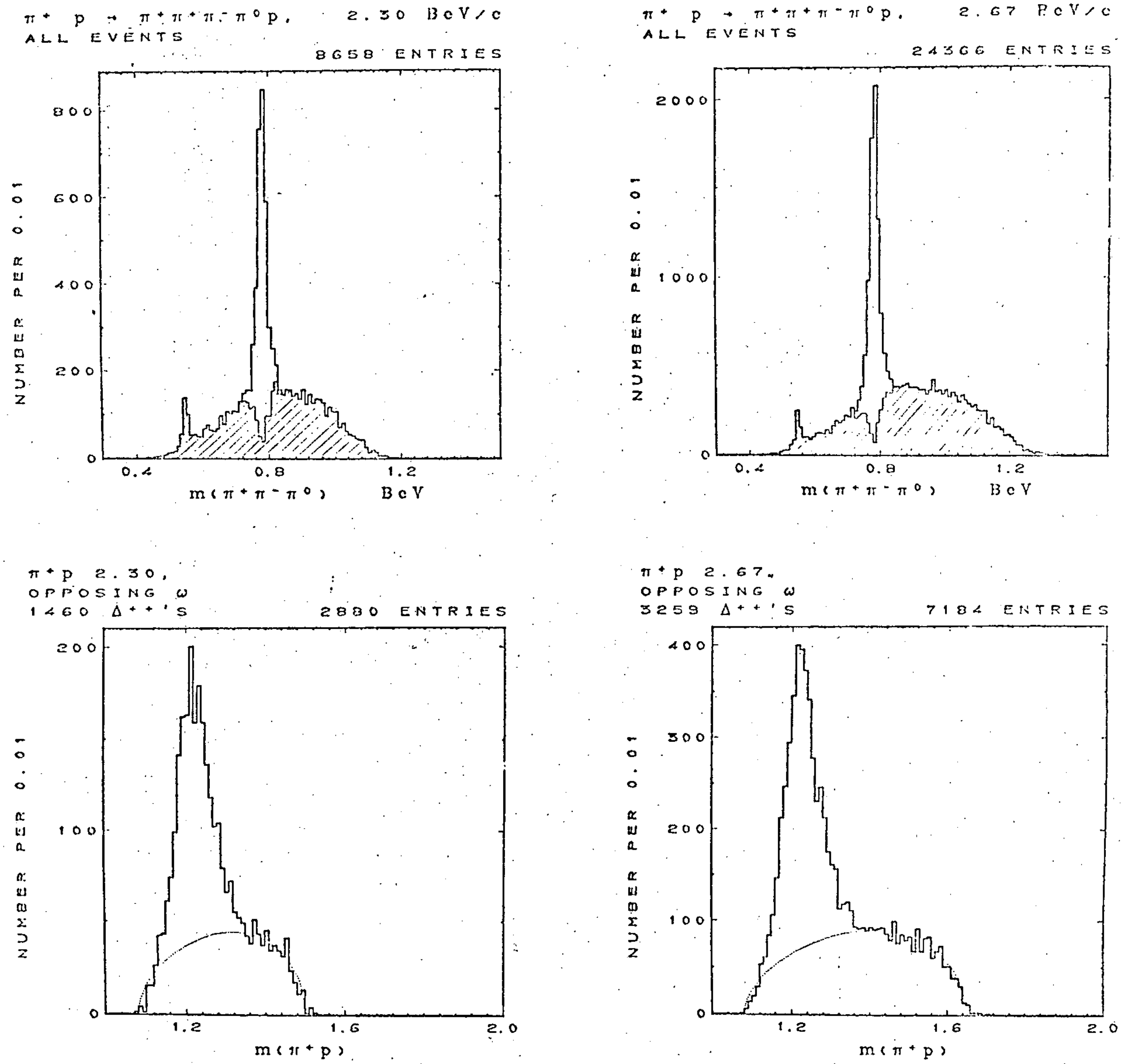
π⁺ p → π⁺π⁺π⁻π⁰p, 2.30 BeV/c
ALL EVENTS
8658 ENTRIES
NUMBER PER 0.01
m(π⁺π⁻π⁰) BeV
π⁺ p → π⁺π⁺π⁻π⁰p, 2.67 BeV/c
ALL EVENTS
24366 ENTRIES
NUMBER PER 0.01
m(π⁺π⁻π⁰) BeV
π⁺p 2.30,
OPPOSING ω
1460 Δ⁺⁺'S
2880 ENTRIES
NUMBER PER 0.01
m(π⁺p)
π⁺p 2.67,
OPPOSING ω
3259 Δ⁺⁺'S
7184 ENTRIES
NUMBER PER 0.01
m(π⁺p)

Fig. 1

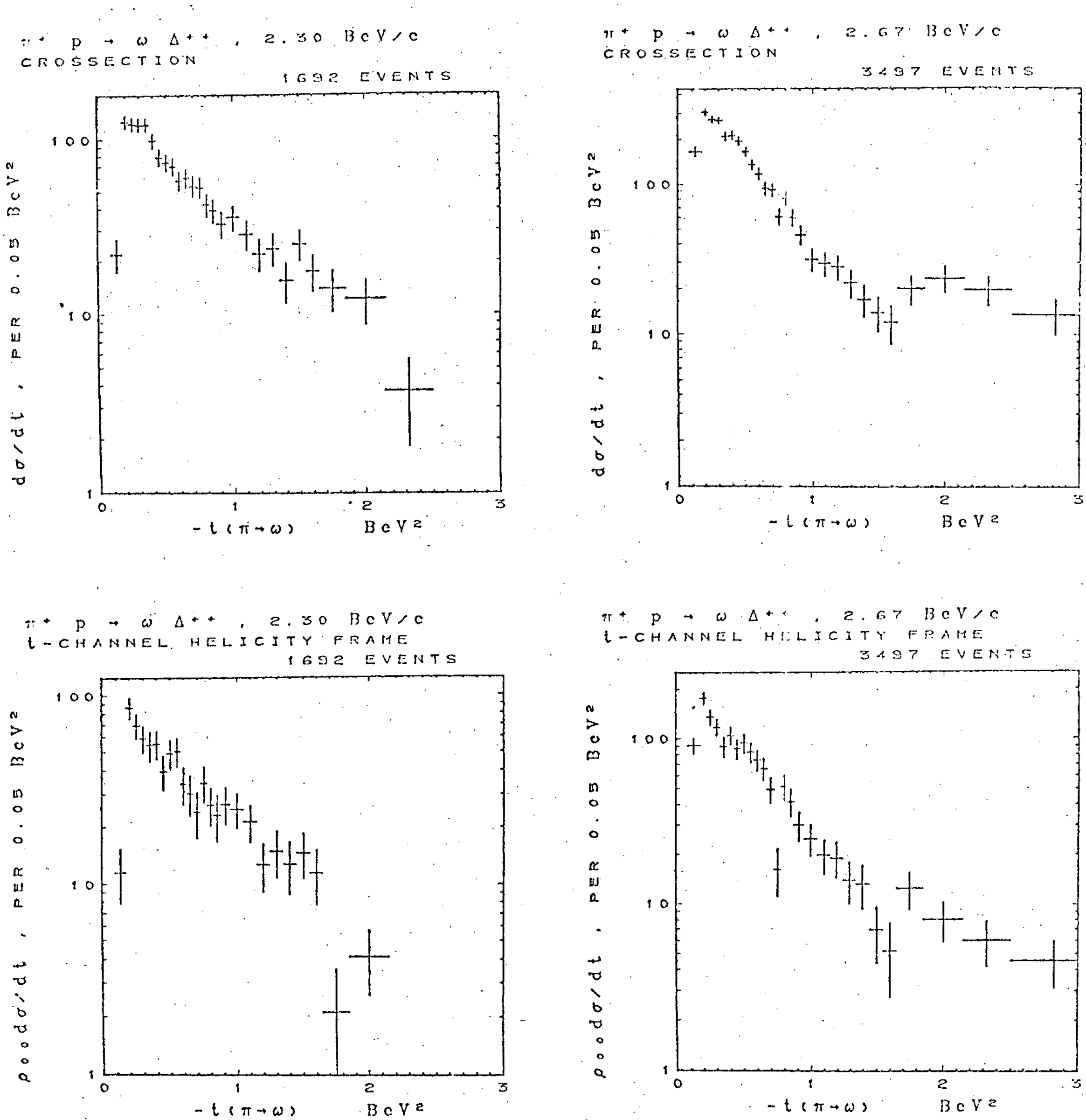
π+ p → ω Δ++ , 2.30 BeV/c
CROSSECTION
1692 EVENTS
dσ/dt , PER 0.05 BeV²
-t(π→ω) BeV²
π+ p → ω Δ++ , 2.67 BeV/c
CROSSECTION
3497 EVENTS
dσ/dt , PER 0.05 BeV²
-t(π→ω) BeV²
π+ p → ω Δ++ , 2.30 BeV/c
t-CHANNEL HELICITY FRAME
1692 EVENTS
ρ00dσ/dt , PER 0.05 BeV²
-t(π→ω) BeV²
π+ p → ω Δ++ , 2.67 BeV/c
t-CHANNEL HELICITY FRAME
3497 EVENTS
ρ00dσ/dt , PER 0.05 BeV²
-t(π→ω) BeV²

Fig. 2

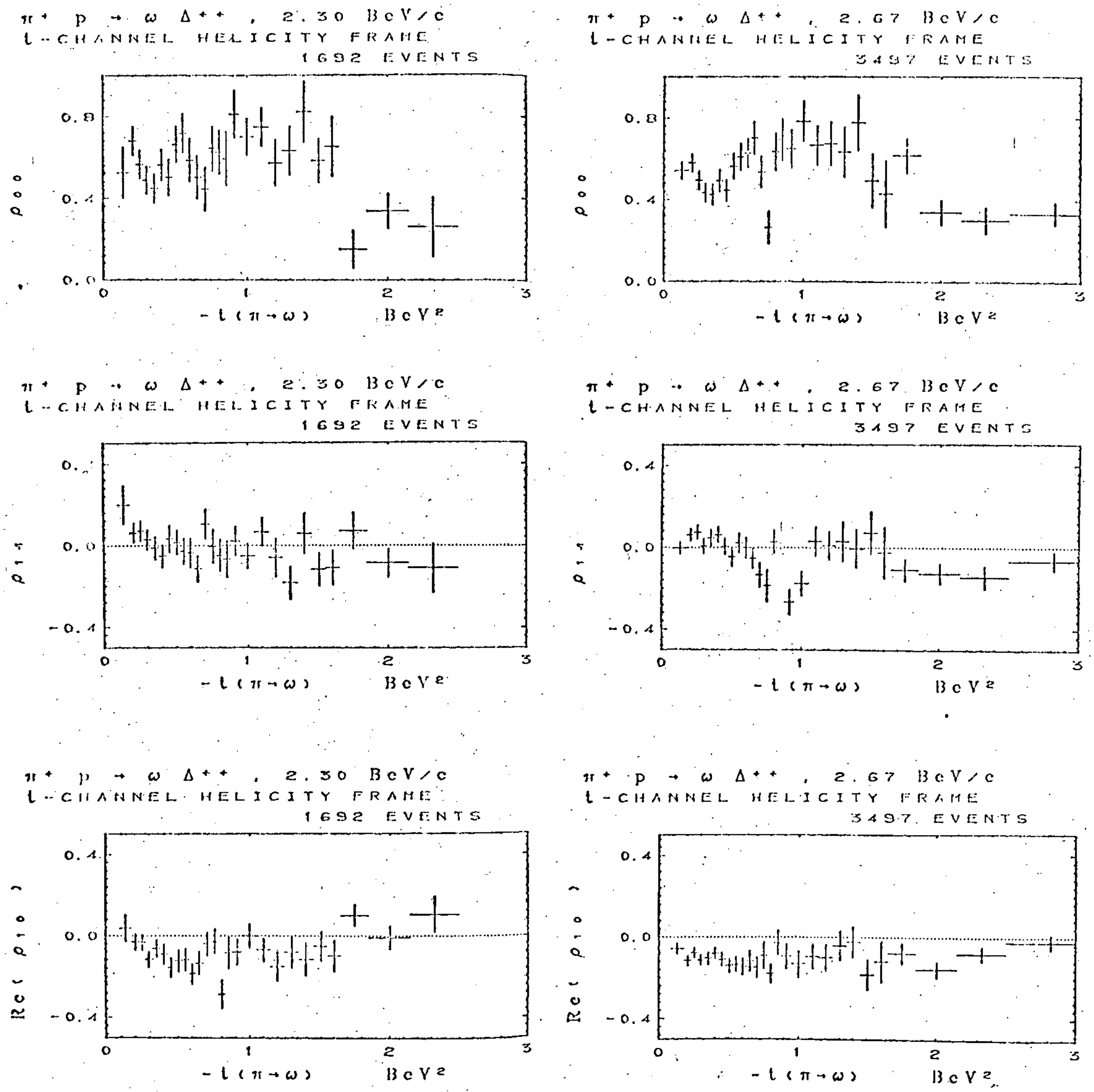

π+ p → ω Δ++ , 2.30 BeV/c
t-CHANNEL HELICITY FRAME
1692 EVENTS
ρ00
-t(π→ω) BeV²
π+ p → ω Δ++ , 2.67 BeV/c
t-CHANNEL HELICITY FRAME
3497 EVENTS
ρ00
-t(π→ω) BeV²
π+ p → ω Δ++ , 2.30 BeV/c
t-CHANNEL HELICITY FRAME
1692 EVENTS
ρ1-1
-t(π→ω) BeV²
π+ p → ω Δ++ , 2.67 BeV/c
t-CHANNEL HELICITY FRAME
3497 EVENTS
ρ1-1
-t(π→ω) BeV²
π+ p → ω Δ++ , 2.30 BeV/c
t-CHANNEL HELICITY FRAME
1692 EVENTS
Re(ρ10)
-t(π→ω) BeV²
π+ p → ω Δ++ , 2.67 BeV/c
t-CHANNEL HELICITY FRAME
3497 EVENTS
Re(ρ10)
-t(π→ω) BeV²


Fig. 3

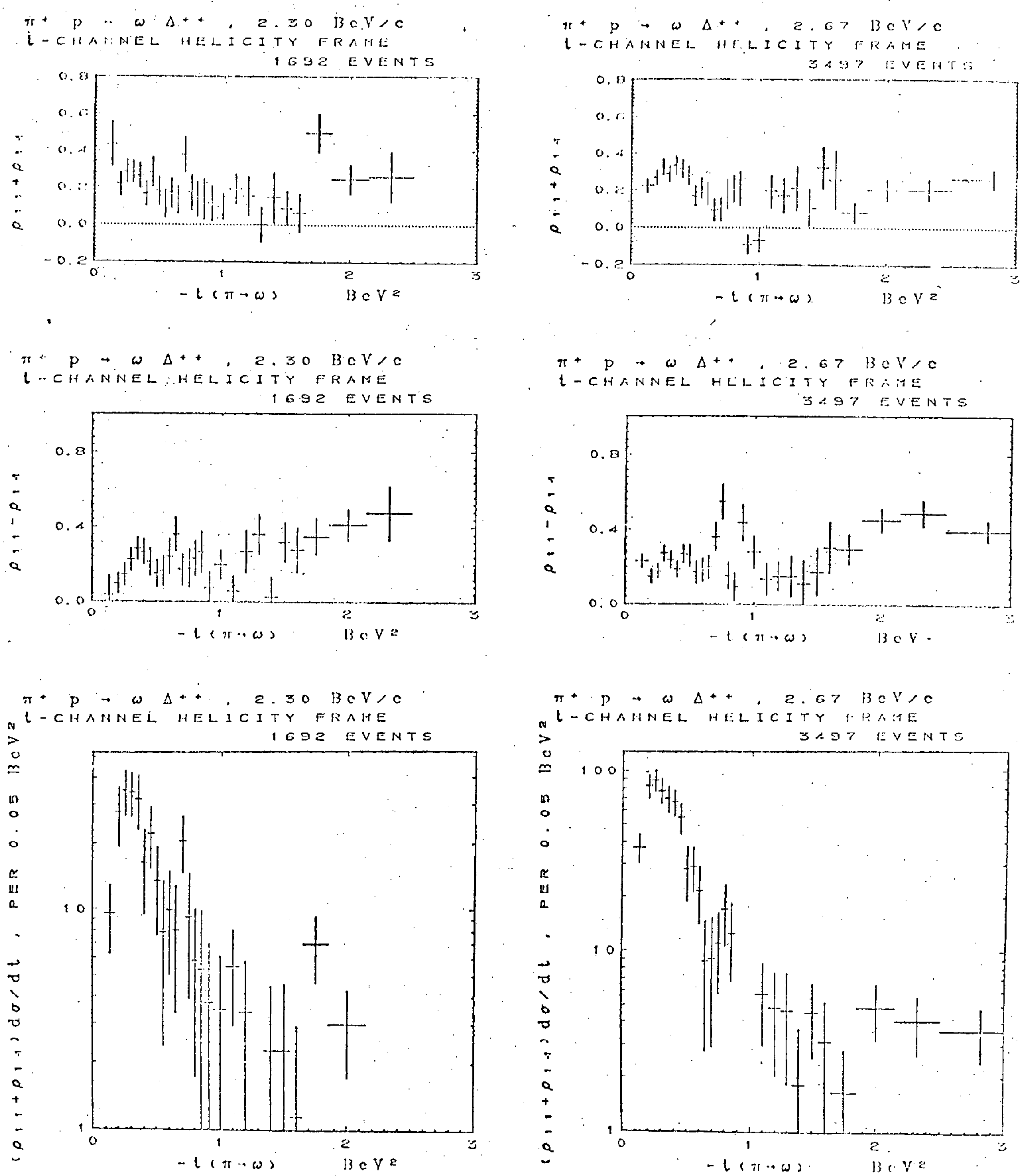
π⁺ p → ω Δ⁺⁺ , 2.30 BeV/c
t-CHANNEL HELICITY FRAME
1692 EVENTS
π⁺ p → ω Δ⁺⁺ , 2.67 BeV/c
t-CHANNEL HELICITY FRAME
3497 EVENTS
ρ11+ρ1-1
ρ11−ρ1-1
(ρ11+ρ1-1) dσ/dt , PER 0.05 BeV²
−t (π→ω)   BeV²

Fig. 4

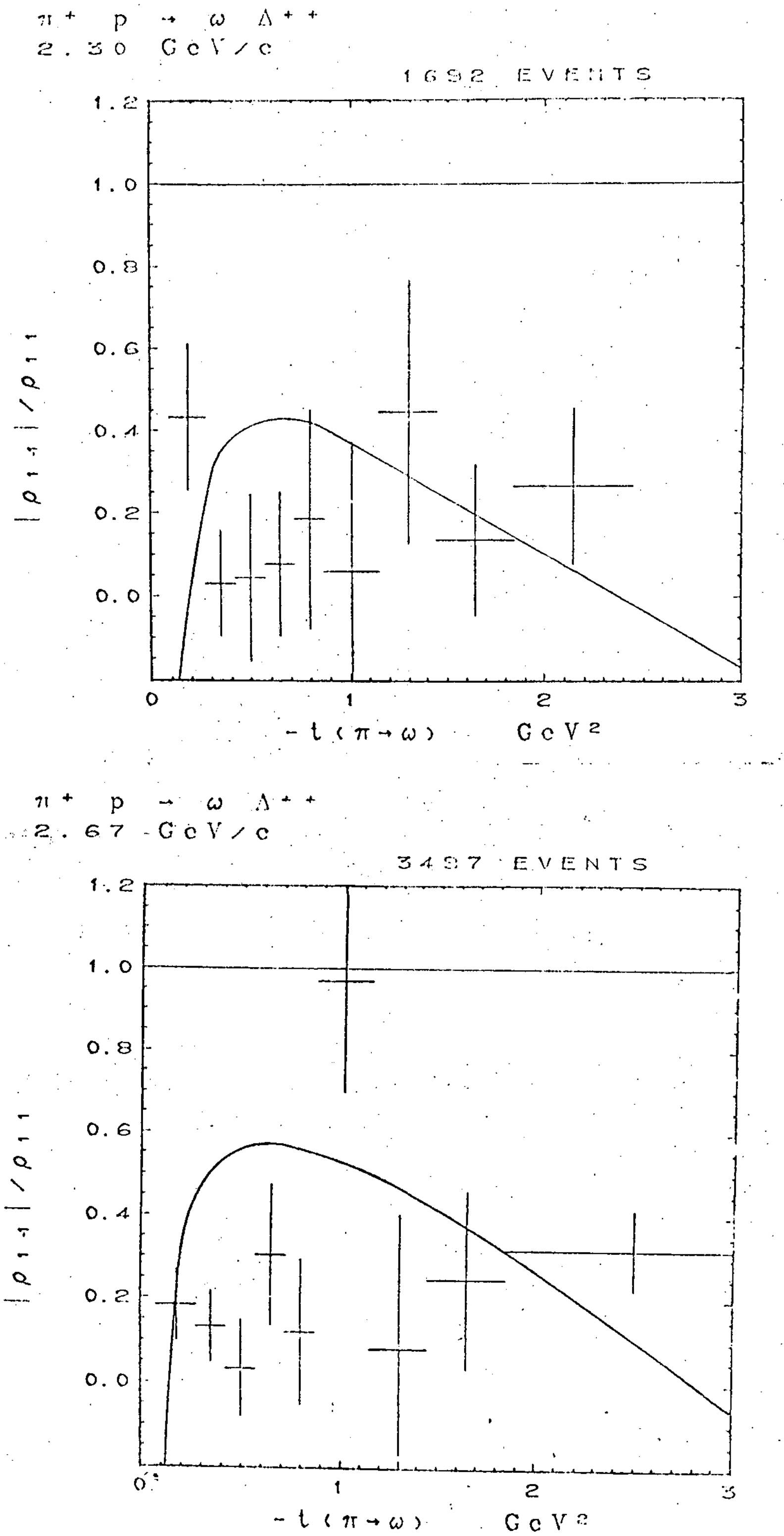
π + p → ω Δ ++
2.30 GeV/c
1692 EVENTS
1.2
1.0
0.8
0.6
0.4
0.2
0.0
|ρ1-1|/ρ11
0
1
2
3
-t (π→ω) GeV²
π + p → ω Δ ++
2.67 GeV/c
3497 EVENTS
1.2
1.0
0.8
0.6
0.4
0.2
0.0
|ρ1-1|/ρ11
0
1
2
3
-t (π→ω) GeV²

Fig. 5

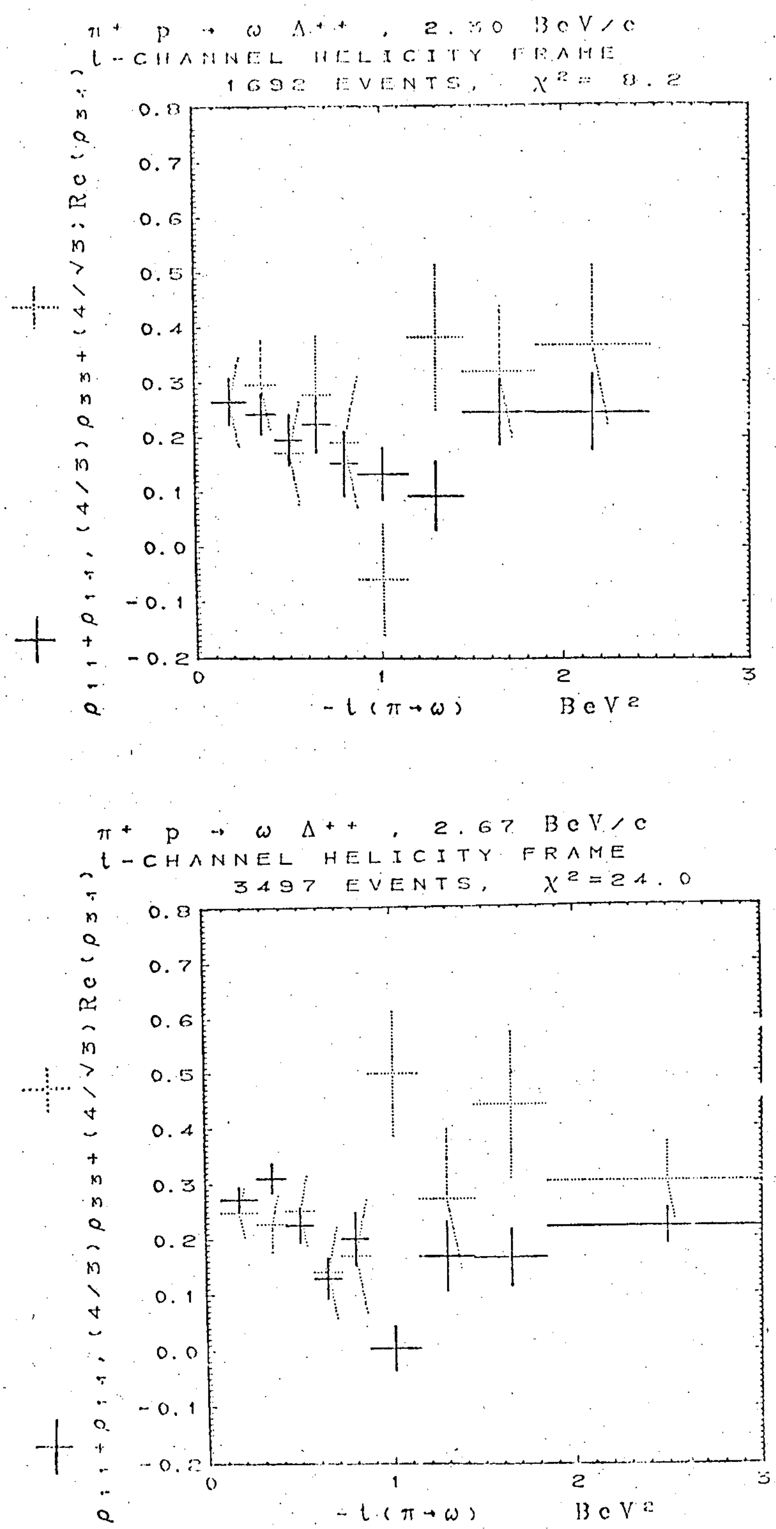
π+ p → ω Δ++ , 2.30 BeV/c
t-CHANNEL HELICITY FRAME
1692 EVENTS, χ² = 8.2
ρ11+ρ1-1, (4/3)ρ33+(4/√3)Re(ρ31)
0.8
0.7
0.6
0.5
0.4
0.3
0.2
0.1
0.0
-0.1
-0.2
0
1
2
3
-t(π→ω) BeV²
π+ p → ω Δ++ , 2.67 BeV/c
t-CHANNEL HELICITY FRAME
3497 EVENTS, χ² = 24.0
ρ11+ρ1-1, (4/3)ρ33+(4/√3)Re(ρ31)
0.8
0.7
0.6
0.5
0.4
0.3
0.2
0.1
0.0
-0.1
-0.2
0
1
2
3
-t(π→ω) BeV²

Fig. 6

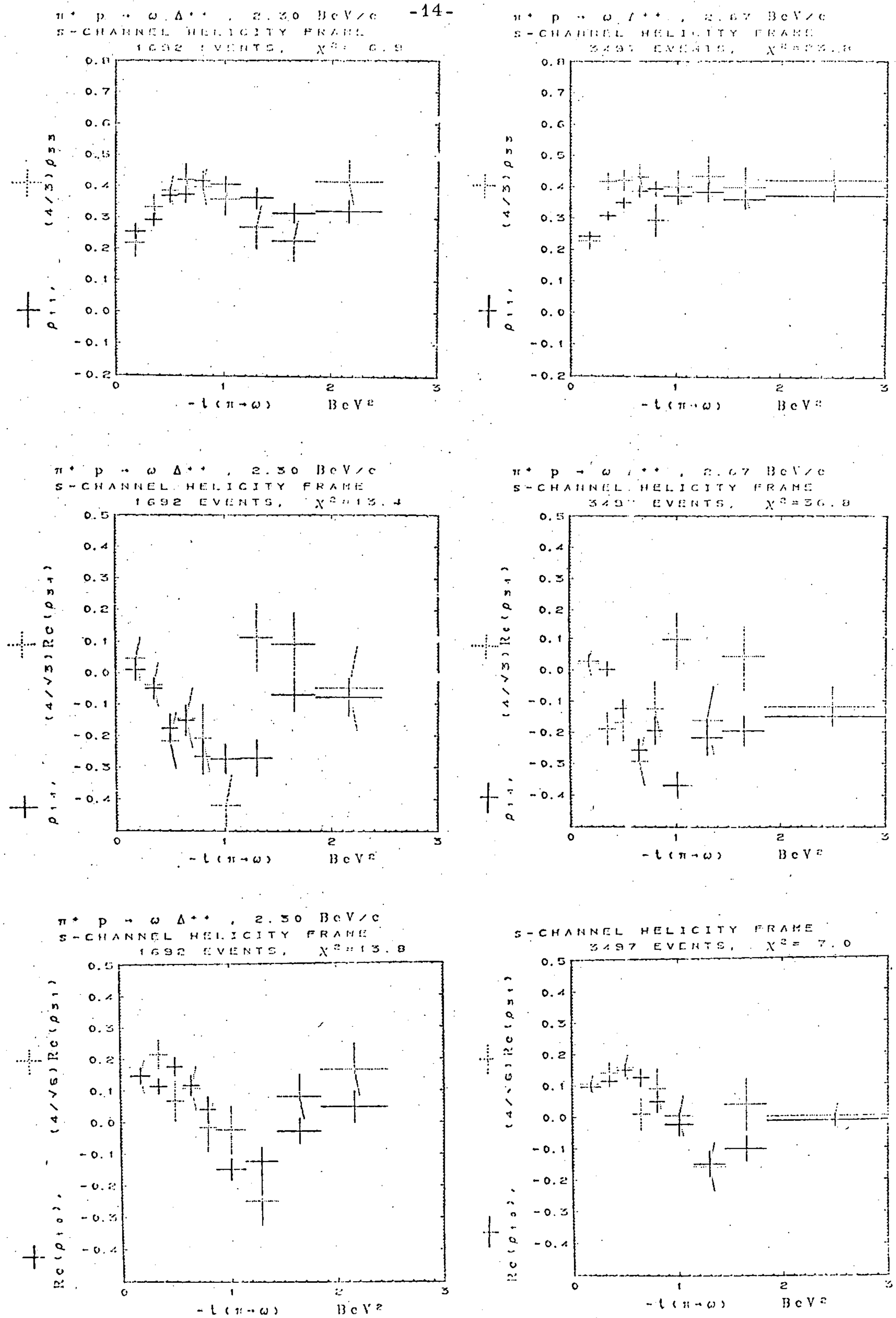
π⁺ p → ω Δ⁺⁺ , 2.30 BeV/c
S-CHANNEL HELICITY FRAME
1692 EVENTS, χ²= 6.9
S-CHANNEL HELICITY FRAME
(4/3)ρ33
ρ11,
-t(π→ω) BeV²
π⁺ p → ω Δ⁺⁺ , 2.30 BeV/c
S-CHANNEL HELICITY FRAME
1692 EVENTS, χ²=13.4
(4/√3)Re(ρ34)
ρ14,
-t(π→ω) BeV²
π⁺ p → ω Δ⁺⁺ , 2.30 BeV/c
S-CHANNEL HELICITY FRAME
1692 EVENTS, χ²=13.8
(4/√6)Re(ρ31)
Re(ρ10),
-t(π→ω) BeV²
S-CHANNEL HELICITY FRAME
3497 EVENTS, χ²= 7.0

Fig. 7

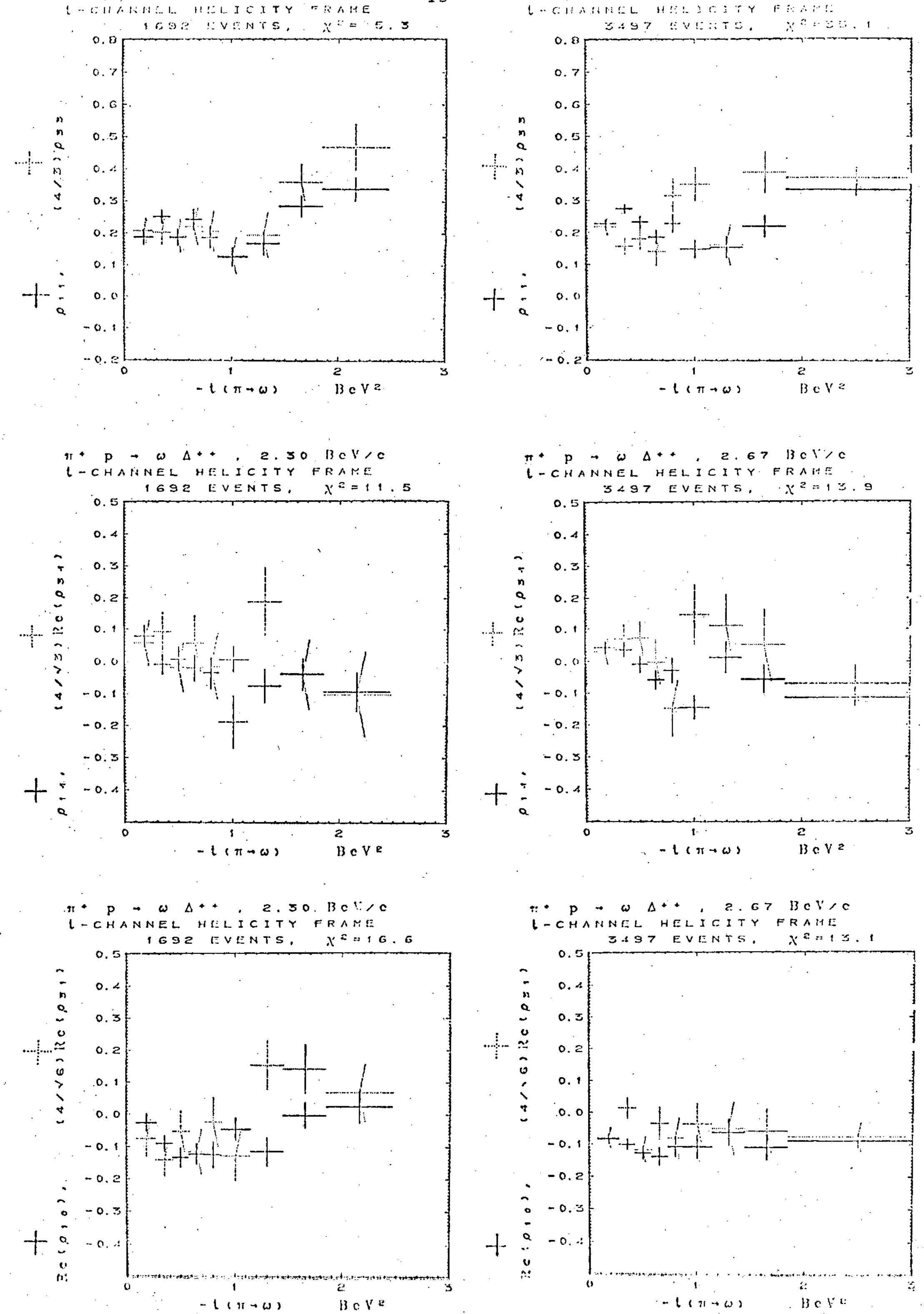

π⁺ p → ω Δ⁺⁺ , 2.30 BeV/c
t-CHANNEL HELICITY FRAME
1692 EVENTS, χ² = 5.3
π⁺ p → ω Δ⁺⁺ , 2.67 BeV/c
t-CHANNEL HELICITY FRAME
3497 EVENTS
ρ₁₁, (4/3) ρ₃₃
-t (π→ω) BeV²
π⁺ p → ω Δ⁺⁺ , 2.30 BeV/c
t-CHANNEL HELICITY FRAME
1692 EVENTS, χ² = 11.5
π⁺ p → ω Δ⁺⁺ , 2.67 BeV/c
t-CHANNEL HELICITY FRAME
3497 EVENTS, χ² = 13.9
ρ₁₄, (4/√3) Re(ρ₃₄)
-t (π→ω) BeV²
π⁺ p → ω Δ⁺⁺ , 2.30 BeV/c
t-CHANNEL HELICITY FRAME
1692 EVENTS, χ² = 16.6
π⁺ p → ω Δ⁺⁺ , 2.67 BeV/c
t-CHANNEL HELICITY FRAME
3497 EVENTS, χ² = 13.1
Re(ρ₁₀), (4/√6) Re(ρ₃₁)
-t (π→ω) BeV²


Fig. 8

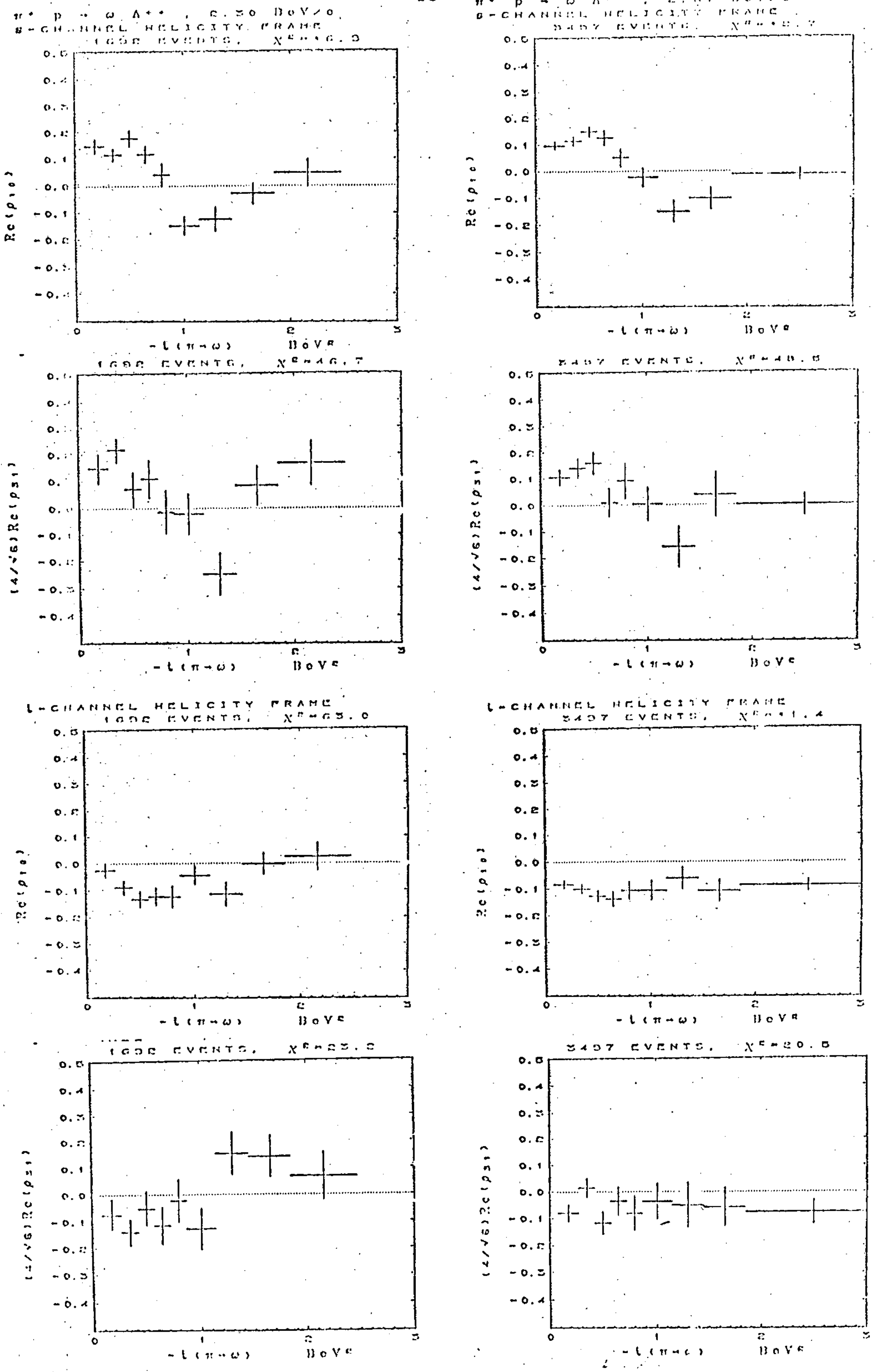
s-CHANNEL HELICITY FRAME
t-CHANNEL HELICITY FRAME
t-CHANNEL HELICITY FRAME
-t(π→ω)
GeV²

Fig. 9

## LEGAL NOTICE